Available online at www.sciencedirect.com

ScienceDirect

Journal of the European Ceramic Society 30 (2010) 1513–1518

www.elsevier.com/locate/jeurceramsoc

Effect of the sintering additive content on the non-protective oxidation behaviour of pressureless liquid-phase-sintered α-SiC in air

F. Rodríguez-Rojas, A.L. Ortiz*, O. Borrero-López, F. Guiberteau

Departamento de Ingeniería Mecánica, Energética y de los Materiales, Escuela de Ingenierías Industriales, Universidad de Extremadura, 06071 Badajoz, Spain

Received 10 August 2009; received in revised form 30 September 2009; accepted 14 October 2009
Available online 27 November 2009

Abstract

The long-term oxidation resistance of pressureless liquid-phase-sintered (PLPS) α-SiC was investigated as a function of the content of sintering additive (in particular, YAG) at 1500 °C in air. It is shown that, regardless of the vol.% YAG, the oxidation is passive at that high temperature, with a kinetics given by the paralinear-rate law. This is because the oxide scales grow due to oxidation of the SiC grains, but recede due to the formation of a eutectic phase and to the carbothermal reduction of YAG. It is also shown that the oxidation resistance of PLPS SiC decreases markedly with increasing vol.% YAG, an effect that is especially marked above 7.3 vol.% YAG where a change in oxidation behaviour occurs. Thus, while up to 7.3 vol.% YAG the PLPS SiC ceramics gain mass during the entire oxidation process (500 h) because the oxide scales are at least semi-protective, from 11.1 vol.% YAG onwards the PLPS SiC ceramics first gain mass and then lose mass linearly over oxidizing time because the oxide scales are non-protective. Finally, implications for the design of PLPS SiC ceramics that can tolerate prolonged exposures at high temperatures in air are discussed.

Keywords: SiC; Liquid-phase sintering; Oxidation

1. Introduction

There is growing interest in investigating the oxidation behaviour of non-oxide ceramics, since this is a major cause of their degradation in high-temperature applications in air, and therefore is a critical design issue.[1] In this context, the oxidation resistance of pressureless liquid-phase-sintered SiC (PLPS SiC), an important low-cost structural ceramic [2–11, and references therein] with an emerging potential as an electro-ceramic for functional applications,[12–14] has yet to be sufficiently studied with respect to its dependence on the processing variables under an ample range of oxidation conditions.

The key to the processing of PLPS SiC is the use of oxide sintering additives, the most widely used of which is a combination of Al_2O_3 and Y_2O_3 at relative concentrations of between 5 and 20 vol.%.[2,15,16] Liu's study of the oxidation of PLPS α-SiC with 5, 10, and 20 wt.% of Al_2O_3–Y_2O_3[17] found that the oxidation resistance decreases with increasing wt.% of sintering aids, and observed a fall in the oxidation activation energy given empirically by the expression E_a (kJ/mol) = 139(2) − 2.4(1) wt.% However, Liu's work explored only the less testing oxidation regime because the most hostile oxidation condition employed was an exposure to air at 1350 °C for 100 h, and under these "mild" conditions the oxidation is passive and the oxide scales are protective (the rate-limiting mechanism is the inward diffusion of molecular oxygen through the oxide scale).[17] Beyond this oxidation regime, the importance of the sintering aid content has yet to be determined, even though this helps in the tailoring of PLPS SiC microstructures for oxidation-resistance applications.

With this in mind, the present work was aimed at extending Liu's work to far more hostile oxidation conditions, in particular analyzing the influence of the Y_2O_3–Al_2O_3 content on the oxidation resistance of PLPS SiC at 1500 °C for up to 500 h of oxidation. This type of study is critical if PLPS SiC is to be utilized routinely in air or can come into contact accidentally with air at high temperatures.

2. Experimental procedure

Fully dense PLPS SiC ceramics were prepared from six powder batches each containing α-SiC (UF-15, H.C. Starck,

---

* Corresponding author.
E-mail address: alortiz@unex.es (A.L. Ortiz).

0955-2219/$ – see front matter © 2009 Elsevier Ltd. All rights reserved.
doi:10.1016/j.jeurceramsoc.2009.10.008

Goslar, Germany), plus Al_2O_3 (AKP-30, Sumitomo Chemical Company, NY) and Y_2O_3 (Fine Grade, H.C. Starck, Goslar, Germany) in 5:3 molar ratio as additives. The maximum oxygen content in the α-SiC powder is 1.5 wt.%, as reported by the manufacturer. The relative amounts of SiC and ($5Al_2O_3 + 3Y_2O_3$) in each of the powder batches were varied to yield PLPS SiC ceramics with 3.6, 7.3, 11.1, 15.0, 19.1, and 23.2 vol.% YAG after sintering (abbreviated hereafter as SiC–xYAG, where x is the vol.% YAG). Compacts were made by uniaxial pressing (C, Carver Inc., Wabash, IN, USA) at 50 MPa, followed by isostatic pressing (CP360, AIP, Columbus, OH, USA) at 350 MPa. Pressureless sintering was performed in a graphite furnace (1000-3560-FP20, Thermal Technology Inc., Santa Rosa, CA, USA) at 1950 °C for 2 h in a flowing Ar-gas atmosphere.

The long-term oxidation tests were carried out using specimens of 1 cm × 1 cm × 1 cm with all their faces diamond-polished to a 1-μm finish. The tests were performed in a bottom-loading furnace at 1500 °C in air, for times in the range 0–500 h. To avoid external contamination during the oxidation tests, the furnace was previously carefully cleaned, and the samples rested on high-purity CVD SiC plates. The oxidation curves in the form specific mass-change–oxidizing time were constructed by placing the samples in the furnace interior already pre-heated empty to 1500 °C, and then, at intervals, removing them from the furnace, cold-weighing to ±0.0001 g (unstuck from the plates), and returning them to the furnace for further oxidation. The oxidation tests were terminated when an accumulated oxidizing time of 500 h was reached. The use of CVD SiC plates as holders is not likely to influence the oxidation behaviour because their oxidation-rate constants are two orders of magnitude lower than those of the PLPS SiC specimens, and because air can still reach the bottom surface of the specimens since the specimen/plate contacts are not airtight.

The as-processed and selected oxidized samples were examined at low-magnifications with a digital camera (DMZ FZ-18, Panasonic, Spain) and at high-magnifications with a scanning electron microscope (SEM; S-3600N, Hitachi, Japan). The SEM observations of the as-processed samples were made on cross-sectional specimens polished to a 1-μm finish, plasma etched with $CF_4 + 4\%\ O_2$ gas for 2 h, and metallized with Pt, and the SEM examinations of the oxidized samples were made on plane-view specimens only metallized and on cross-sectional specimens polished to a 1-μm finish and also metallized. In all cases the micrographs were taken at 30 kV with secondary electrons.

3. Results

Fig. 1 shows representative SEM images of the microstructure of the PLPS SiC ceramics prepared with lowest (*i.e.*, 3.6 vol.%) and highest (*i.e.*, 23.2 vol.%) YAG contents. As can be observed, the size (0.8 μm) and aspect ratio (1.4) of the SiC grains are both independent of the YAG vol.%, a fact that the SEM analyses on the rest of the materials (*i.e.*, those with 7.3, 11.1, 15.0, and 19.1 vol.% YAG) confirmed. This similitude in the grain morphology and size has been observed before,[7,16] and has been attributed to the coarsening in PLPS α-SiC fabricated in Ar atmosphere being controlled by an interface reaction, not by diffusion through the liquid phase.[16]

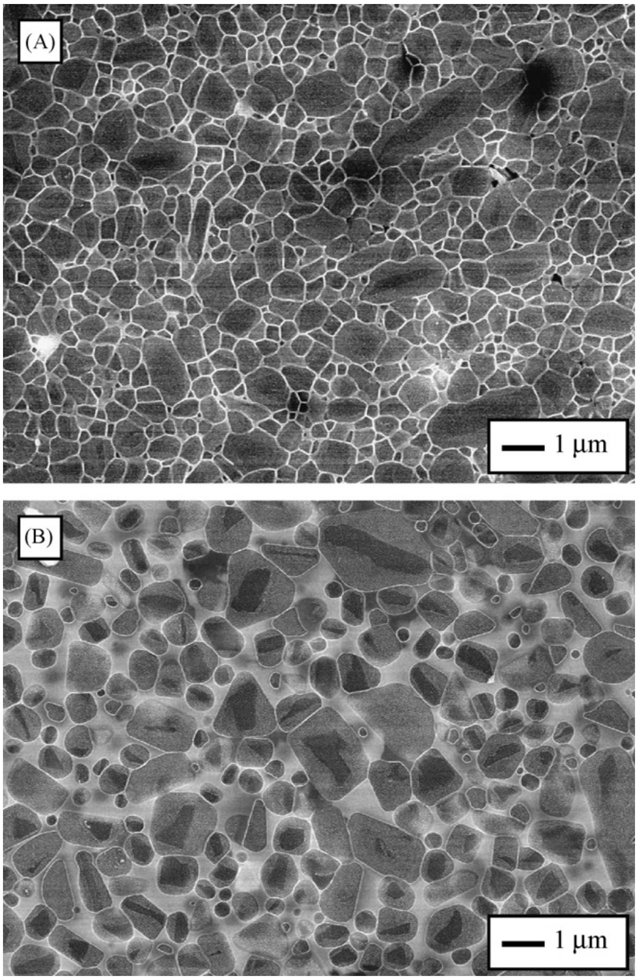

Fig. 1. SEM micrographs of the PLPS SiC ceramics fabricated with: (A) 3.6 vol.% YAG, (B) 23.2 vol.% YAG. The dark regions are the SiC grains and the light region is the YAG phase. The core–shell substructure within the SiC grains is visible in the micrographs due to differential plasma-etching.

Fig. 2 presents the oxidation curves (1500 °C in air) for the six ceramics prepared in this study, which demonstrate that the oxi-

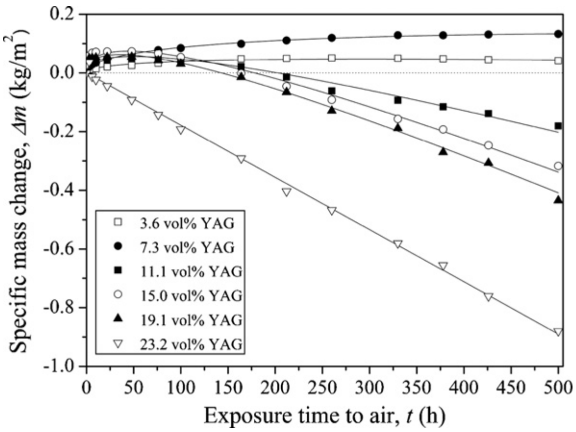

Fig. 2. Oxidation curves in air at 1500 °C of the six PLPS SiC ceramics prepared in this study. The points are the experimental data, and the solid lines are the paralinear oxidation kinetics models (discussed in the text).

Fig. 3. Surface appearance as a function of vol.% YAG for the PLPS SiC ceramics after oxidation in air at 1500 °C for 22, 260, and 500 h.

dation resistance of PLPS SiC decreases notably with increasing YAG content. As can be observed, when the YAG content is low (*i.e.*, 3.6 and 7.3 vol.%) the PLPS SiC ceramics gain mass during the entire oxidation period, with a kinetics that does not obey the parabolic-rate law because the $(\Delta m_s)^2 - t$ relationship is not completely linear over the whole t range but exhibits a certain concavity (not shown). Furthermore, SiC–7.3YAG gains more mass than SiC–3.6YAG. This type of oxidation curve reflects the existence of a mass loss process superimposed on a dominant mass gain process.[1,18] The mass gain is due to the formation of solid oxidation products and its kinetics follows the parabolic-rate law, whereas the mass loss is due to the formation of liquid and/or gaseous oxidation products that leave the sample, and its kinetics obeys the linear-rate law. It can also be observed in Fig. 2 that when the YAG content is high (*i.e.*, ≥11.1 vol.%) the PLPS SiC ceramics start first by gaining mass and then lose mass in a linear fashion. Moreover, the greater the YAG content, the earlier the transition from mass gain to mass loss and the greater the slope of the negative linear stretch of the curve. This type of two-stage curve oxidation is also due to the superposition of mass gain and loss processes.[1,18–21] The important difference is that in this latter case at a certain equilibrium thickness a steady state is reached at which the oxide scale grows and recedes at the same rate.[1,18]

Fig. 3 compares low-magnification optical macrographs of the six PLPS SiC ceramics at different stages of the oxidation test (*i.e.*, 22, 260, and 500 h at 1500 °C in air). The marked effect of the YAG vol.% on the oxidation resistance of PLPS SiC is again very evident. While SiC–3.6YAG maintains a high degree of surface integrity, SiC–7.3YAG shows evident signs of surface degradation, and the samples with higher YAG content do not survive to the oxidation tests and are consumed progressively. The oxide scale in SiC–3.6YAG is flat, smooth, and compact. The SEM observations reveal that this scale is composed of large crystals embedded in a glassy matrix with some pores (Fig. 4A), and that has a relatively uniform thickness of about 20 μm (Fig. 4B). The oxide scale in SiC–7.3YAG is rougher, and has melted and partially flowed out. Finally, surfaces of the PLPS SiC ceramics with 11.1, 15.0, 19.1, and 23.2 vol.% YAG are highly blistered, resembling ceramic foams. The SEM examinations of SiC–23.2YAG show that the foam layer is formed by huge ceramic bubbles with large holes (Fig. 5A), and that beneath the foam layer there is an oxide scale whose thickness varies between a few tens and hundreds of microns depending on the location (Fig. 5B).

4. Discussion

The results presented above indicate that the high-temperature oxidation of PLPS SiC is passive, not active, regardless of the vol.% YAG. Strictly, oxidation is defined as passive if a condensed phase forms on the sample surface in contact with the oxidant species, independently of whether it is protective or not or of whether the sample gains or loses mass.[1] On the contrary, oxidation is defined as active if such a condensed phase does not form because all oxidation products are volatile, resulting then irremediably in mass loss due to the escape of the gaseous species.[1] Thus, the observation of oxide scales in the cross-sectional SEM images (Figs. 4B and 5B) indicates that the oxidation is in all cases passive. Furthermore, it is non-protective because its rate-controlling mechanism is not diffusion through the oxide scale since none of the oxidation kinetics obeys the parabolic-rate law (Fig. 2). However, whereas it is very clear that the oxide scales do not offer protection against the oxidation when the YAG content is high (*i.e.*, ≥11.1 vol.%) because these samples eventually lose mass linearly over the oxidizing time, the oxide scales can nevertheless be considered as semi-protective when the YAG content is low (*i.e.*, 3.6 and 7.3 vol.%)

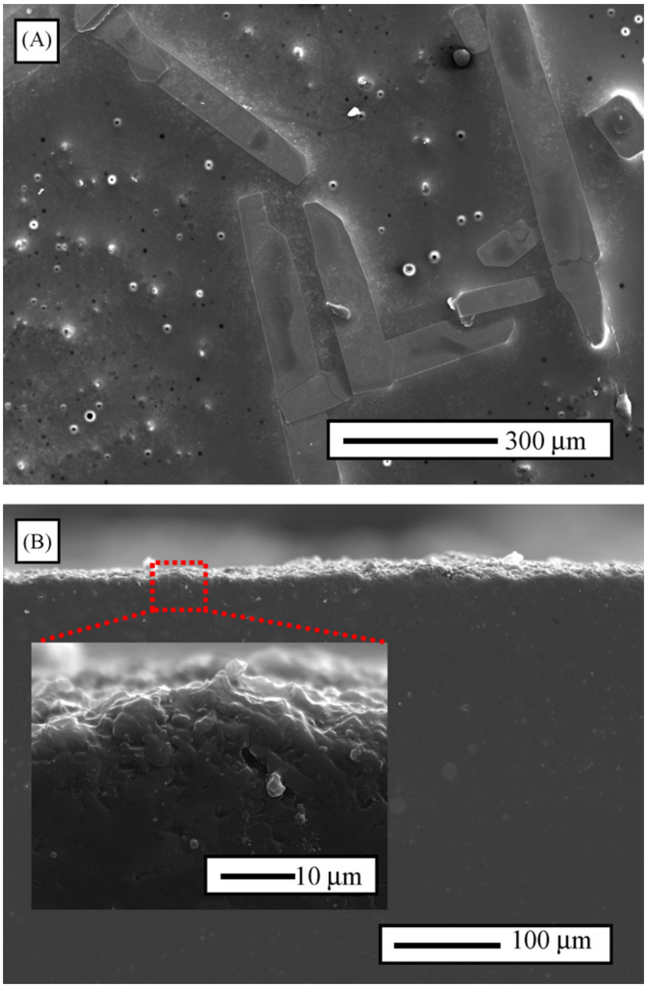

Fig. 4. SEM micrographs of the surface of the PLPS SiC ceramic with 3.6 vol.% YAG after oxidation at 1500 °C in air for 500 h: (A) plane-view image and (B) cross-sectional image.

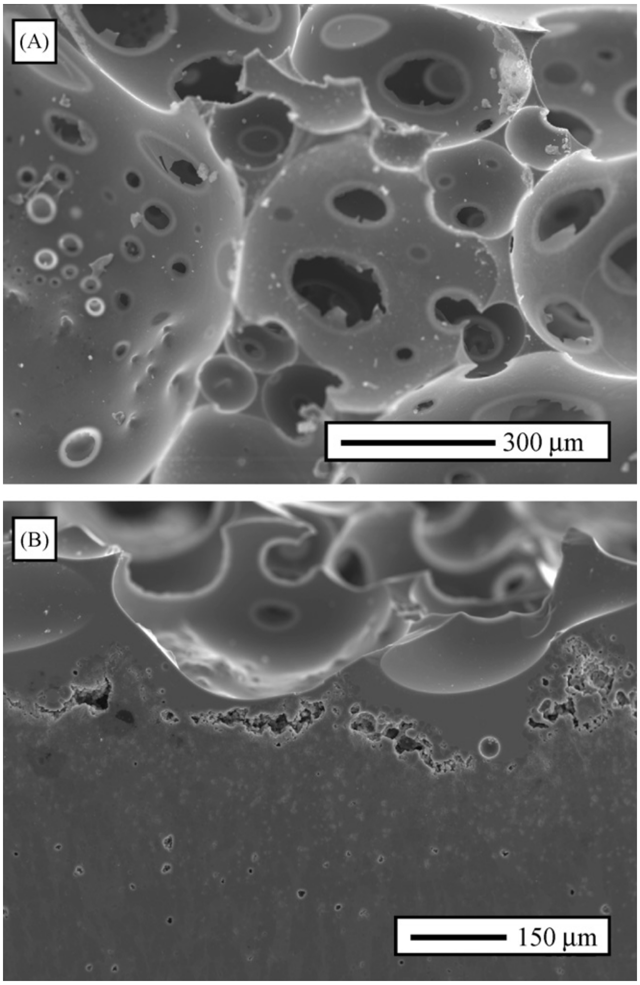

Fig. 5. SEM micrographs of the surface of the PLPS SiC ceramic with 23.2 vol.% YAG after oxidation at 1500 °C in air for 500 h: (A) plane-view image and (B) cross-sectional image.

because the deviation from the parabolic-rate law is not very marked and these two samples at least gain mass during the entire oxidizing period (*i.e.*, 500 h).

The oxidation kinetics of the six PLPS SiC ceramics can be modeled analytically using the paralinear-rate law, which incorporates two terms, one positive for the growth of the oxide scale and the other negative for its recession[a]:

$$\Delta m_s = \sqrt{k_p t} - k_l t \tag{1}$$

where k_p and k_l are the parabolic and linear-rate constants, respectively. Fig. 2 shows the good agreement existing between the model and experimental curves, and Fig. 6 plots the corresponding parabolic and linear-rate constants as a function of the YAG vol.%. It can be seen from Fig. 7 that for low YAG contents (*i.e.*, 3.6 and 7.3 vol.%) the oxidation kinetics are dominated by the positive parabolic term ($k_l^2 t/k_p < 1$), which is because these oxide scales offer partial protection against the oxidation. Nevertheless, theoretical estimates performed with these

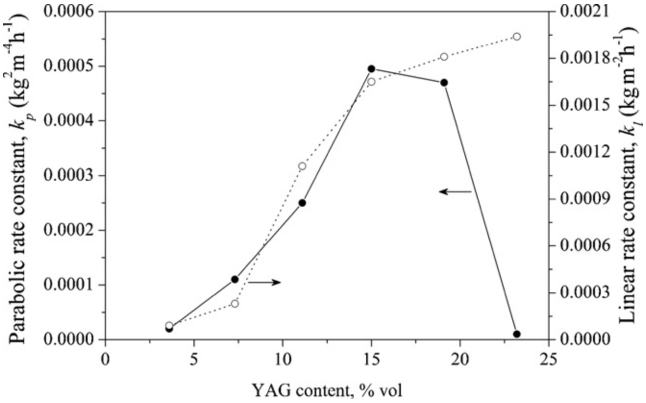

Fig. 6. The rate constants for the paralinear oxidation in air at 1500 °C of the PLPS SiC ceramics as a function of vol.% YAG.

---

[a] Previous studies have shown that indeed the oxidation kinetics of PLPS SiC at high temperatures in air is somewhat more complex, obeying first the arctan-rate law briefly, and then the paralinear-rate law.[22,23] The initial arctan regime is due to the crystallization of the oxide scale during the first moments of the oxidation. However, given that the duration of the arctan regime at 1450 °C is very short, of the order of only a few hours (5 h or less), in the present study the oxidation curves at 1500 °C have been described using the paralinear-rate law exclusively. This approach is justified because the fits captured the oxidation kinetics remarkably well ($\chi_r^2 > 0.98$).

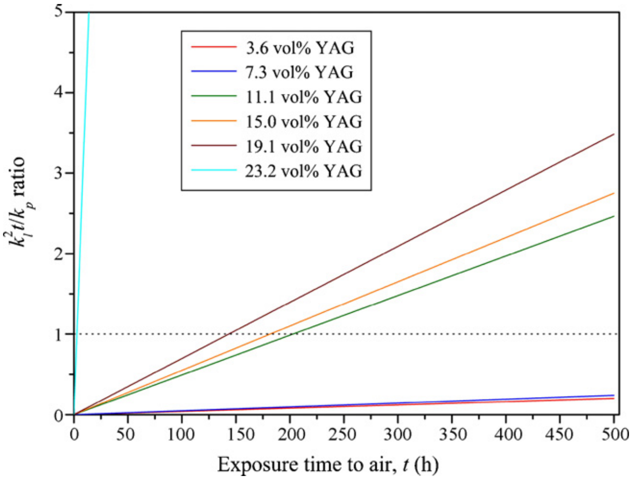

Fig. 7. Plot of k_l^2t/k_p as a function of the oxidizing time for the six PLPS SiC ceramics prepared in this study. The dashed line separates the regions of mass gain ($k_l^2t/k_p < 1$) and mass loss ($k_l^2t/k_p > 1$).

k_p and k_l values indicate that SiC–3.6YAG and SiC–7.3YAG will enter into mass loss at about 2470 and 2080 h, respectively, which is when the corresponding oxide scales become non-protective. Thus, the earlier expected transition to mass loss, together with the higher k_p and k_l values indicate that the oxidation resistance of PLPS SiC decreases with increasing YAG content from 3.6 to 7.3 vol.%. Also, it can be seen in Fig. 7 that for high YAG contents (*i.e.*, ≥11.1 vol.%) there is a first oxidation stretch dominated by the positive parabolic term ($k_l^2t/k_p < 1$), the duration of which shortens as the vol.% YAG increases, followed by a second oxidation stretch dominated by the negative linear term ($k_l^2t/k_p > 1$), the severity of which increases with increasing vol.% YAG. These are because these oxide scales protect at least marginally against the short-term oxidation, but not against the long-term oxidation. Thus, the earlier transition to mass loss (*i.e.*, ~203, 182, 143, and 3 h) and the higher k_l values indicate that the oxidation resistance of PLPS SiC also decreases with increasing YAG content from 11.1 to 23.2 vol.%.

Let us first analyze the origin of the paralinear oxidation of the PLPS SiC ceramics at 1500 °C. Logically, the mass gain term is due to the oxidation of the SiC grains via the reaction

$$2SiC(s) + 3O_2(g) \rightarrow 2SiO_2(s) + 2CO(g) \qquad (2)$$

Note that although this reaction involves a mass loss term (*i.e.*, escape of CO), the net balance leads to mass gain. As for the mass loss term, the optical macrographs (Fig. 3) indicate that this occurs by liquid flow and material volatilization. The low-viscosity liquid is the eutectic phase that the Y_2O_3–Al_2O_3–SiO_2 ternary system has at 1371 °C,[24] where the SiO_2 comes from reaction (2). The volatiles are the gaseous products of reaction (2) and of the carbothermal reduction reaction of YAG:[25]

$$Y_3Al_5O_{12}(s) + 4CO(g) \rightarrow 3YAlO_3(s) + Al_2OC(g) + 3CO_2(g) \qquad (3)$$

where the CO(g) reactant is a product of reaction (2). Since CO(g) forms in the vicinity of YAG (*i.e.*, at the SiC grains), reaction (3) is not controlled by diffusion but by interface reaction, and is thus linear over time. Note that the active oxidation of SiC ($SiC(s) + O_2(g) \rightarrow SiO(g) + CO(g)$, or $SiC(s) + 3O_2(g) \rightarrow 2SiO_2(g) + 2CO(g)$) can be ruled out because this occurs at lower oxygen partial pressure and higher temperature[1] than used in the present study. Thus, the final negative linear stretch of the oxidation curve of the PLPS SiC ceramics with high YAG contents (*i.e.*, ≥11.1 vol.%) seems to indicate that the mass loss term is dominated by escape of the gaseous species.

Consider now the effect of YAG content on the oxidation properties of PLPS SiC. With increasing YAG vol.%, the amount of eutectic phase and the extent of reaction (3) will increase. Since these two factors cause mass loss, they will reinforce each other in degrading the oxidation resistance of PLPS SiC. This is consistent with the experimental observations. As the YAG content increases, net mass loss will occur at a certain YAG vol.% for which reaction (2) is balanced eventually by the formation of the eutectic phase plus reaction (3), representing a clear change in the shape of the oxidation curves because the oxide scales are no longer semi-protective but non-protective. This is also consistent with the experimental observations, which in addition show that such a critical YAG content is between 7.3 and 11.1 vol.%.

To conclude, the present study has thus very interesting implications for the design of PLPS SiC components that can tolerate prolonged exposures at high temperature in air. Indeed, according to the results, the intergranular phase content should be reduced as much as possible for oxidation-resistance applications, and cannot be superior to 7.3 vol.% in the case of YAG. Since one achieves hardly any densification in PLPS SiC by introducing low loads of additives (<3 vol.%) via the classical mechanical mixture of powders, it would be highly desirable to identify new methods of batch preparation that lead to a better dispersion of minimal contents of sintering aids. This must, however, remain for future work.

5. Conclusions

The influence of the sintering additive content (specifically vol.% YAG) on the long-term oxidation behaviour of PLPS SiC in air at 1500 °C was investigated. Based on this study, the following conclusions can be drawn:

(1) The sintering additive content does not affect the nature of the oxidation, which is passive at that high temperature due to the formation of oxide scales.
(2) On the contrary, the sintering additive content conditions notably the high-temperature oxidation resistance of PLPS SiC. Thus, reduction of the sintering aid content as much as possible emerges as a design guideline for oxidation-resistance applications.
(3) Regardless of the sintering additive content, the oxidation kinetics obeys the paralinear-rate law because of the simultaneous growth (oxidation of the SiC grains into SiO_2)

and recession (formation of a eutectic phase and carbothermal reduction of YAG) of the oxide scales. The values of the parabolic and linear-rate constants of the paralinear-rate law are, however, affected markedly by the sintering additive content.

(4) When the sintering additive content is low (*i.e.*, 3.6 and 7.3 vol.% YAG), the oxide scales are semi-protective, and thus the PLPS SiC ceramics gain mass during the entire oxidation period (500 h). When the sintering additive content is high (*i.e.*, ≥11.1 vol.% YAG), the oxide scales are non-protective, and thus PLPS SiC ceramics start first by gaining mass and then lose mass linearly over the oxidizing time.

Acknowledgments

This work was supported by the Ministerio de Ciencia y Tecnología (Government of Spain) under the Grant No. MAT 2007-61609.

References

1. Nickel, K. G., Corrosion of advanced ceramics. Measurement and modelling. *NATO ASI Series, Series E (Applied Sciences)*, *vol. 267*, 1994.
2. Padture, N. P., In situ-toughened silicon-carbide. *J. Am. Ceram. Soc.*, 1994, **77**(2), 519–523.
3. Kim, Y.-W., Mitomo, M. and Nishimura, T., Heat-resistant silicon carbide with aluminum nitride and erbium oxide. *J. Am. Ceram. Soc.*, 2001, **84**(9), 2060–2064.
4. Sigl, L. S., Thermal conductivity of liquid-phase-sintered silicon carbide. *J. Eur. Ceram. Soc.*, 2003, **23**(7), 1115–1122.
5. Ortiz, A. L., Muñoz-Bernabé, A., Borrero-López, O., Domínguez-Rodríguez, A., Guiberteau, F. and Padture, N. P., Effect of sintering atmosphere on the mechanical properties of liquid-phase-sintered SiC. *J. Eur. Ceram. Soc.*, 2004, **24**(10–11), 3245–3249.
6. Meléndez-Martínez, J. J., Castillo-Rodríguez, M., Domínguez-Rodríguez, A., Ortiz, A. L. and Guiberteau, F., Creep and microstructural evolution at high temperature of liquid-phase-sintered silicon carbide. *J. Am. Ceram. Soc.*, 2007, **90**(1), 163–169.
7. Borrero-López, O., Ortiz, A. L., Guiberteau, F. and Padture, N. P., Effect of liquid-phase content on the contact mechanical properties of liquid-phase-sintered α-SiC. *J. Eur. Ceram. Soc.*, 2007, **27**(6), 2521–2527.
8. Borrero-López, O., Ortiz, A. L., Guiberteau, F. and Padture, N. P., Microstructural design of sliding-wear-resistant liquid-phase-sintered SiC: an overview. *J. Eur. Ceram. Soc.*, 2007, **27**(11), 3351–3357.
9. Kim, Y.-W., Mitomo, M. and Nishimura, T., High-temperature strength of liquid-phase-sintered SiC with AlN and RE_2O_3 (RE = Y, Yb). *J. Am. Ceram. Soc.*, 2002, **85**(4), 1007–1009.
10. Nagano, T., Gu, H., Zhan, G.-D. and Mitomo, M., Effect of atmosphere on superplastic deformation behavior in nanocrystalline liquid-phase-sintered silicon carbide with Al_2O_3–Y_2O_3 additions. *J. Mater. Sci.*, 2002, **37**(20), 4419–4424.
11. Castillo-Rodríguez, M., Muñoz, A. and Domínguez-Rodríguez, A., Correlation between microstructure and creep behavior in liquid-phase-sintered α-silicon carbide. *J. Am. Ceram. Soc.*, 2006, **89**(3), 960–967.
12. Sánchez-González, J., Ortiz, A. L., Guiberteau, F. and Pascual-Centenera, C., Complex impedance spectroscopy study of a liquid-phase-sintered α-SiC. *J. Eur. Ceram. Soc.*, 2007, **27**(12–15), 3941–4395.
13. Can, A., McLachlan, D. S., Sauti, G. and Herrmann, M., Relationships between microstructure and electrical properties of liquid-phase-sintered silicon carbide materials using impedance spectroscopy. *J. Eur. Ceram. Soc.*, 2005, **27**(2–3), 1361–1363.
14. Volz, E., Roosen, A., Hartung, W. and Winnacker, A., Electrical and thermal conductivity of liquid phase sintered SiC. *J. Eur. Ceram. Soc.*, 2001, **21**(10–11), 2089–2093.
15. Pujar, V. V., Jensen, R. P. and Padture, N. P., Densification of liquid-phase-sintered silicon carbide. *J. Mater. Sci. Lett.*, 2000, **19**, 1011–1014.
16. Ye, H., Pujar, V. V. and Padture, N. P., Coarsening in liquid-phase-sintered α-SiC. *Acta Mater.*, 1999, **47**(2), 481–487.
17. Liu, D.-M., Oxidation of polycrystalline α-silicon carbide ceramic. *Ceram. Int.*, 1997, **23**(5), 425–436.
18. Wagner, C., Passivity during the oxidation of silicon at elevated temperatures. *J. Appl. Phys.*, 1958, **29**(9), 1295–1297.
19. Tedmon, C. S. J., The effect of oxide volatilization on the oxidation kinetics of Cr and Fe–Cr alloys. *J. Electrochem. Soc.*, 1966, **113**(8), 766–768.
20. Opila, E. J. and Hann Jr., R. E., Paralinear oxidation of CVD SiC in water vapor. *J. Am. Ceram. Soc.*, 1997, **80**(1), 197–205.
21. Nickel, K. G., Ceramic matrix composite corrosion models. *J. Eur. Ceram. Soc.*, 2005, **25**(10), 1699–1704.
22. Rodríguez-Rojas, F., Borrero-López, O., Ortiz, A. L. and Guiberteau, F., Oxidation kinetics of pressureless liquid-phase-sintered α-SiC in ambient air at elevated temperatures. *J. Mater. Res.*, 2008, **23**(6), 1689–1700.
23. Rodríguez-Rojas, F., Ortiz, A. L., Borrero-López, O. and Guiberteau, F., Effect of Ar or N_2 sintering atmosphere on the high-temperature oxidation behaviour of pressureless liquid-phase-sintered α-SiC in air. *J. Eur. Ceram. Soc.*, 2010, **30**(1), 119–128.
24. Kolitsch, U., Seifert, H. J., Ludwig, T. and Aldinger, F., Phase equilibria and crystal chemistry in the Y_2O_3–Al_2O_3–SiO_2 system. *J. Mater. Res.*, 1999, **14**(2), 447–455.
25. Mah, T.-I., Keller, K. A., Sambasivan, S. and Kerans, R. J., High-temperature environmental stability of the compounds in the Al_2O_3–Y_2O_3 system. *J. Am. Ceram. Soc.*, 1997, **80**(4), 874–878.